HOKKAIDO UNIVERSITY

Title	Reexamination of cross sections of the Mo-100(p,2n)Tc-99m reaction
Author(s)	Takacs, S.; Hermanne, A.; Ditroi, F. et al.
Citation	Nuclear Instruments and Methods in Physics Research Section B : Beam Interactions with Materials and Atoms, 347, 26-38 https://doi.org/10.1016/j.nimb.2015.01.056
Issue Date	2015-03-15
Doc URL	https://hdl.handle.net/2115/64705
Rights	c2015, Elsevier. Licensed under the Creative Commons Attribution-NonCommercial-NoDerivatives 4.0 International http://creativecommons.org/licenses/by-nc-nd/4.0/
Rights(URL)	https://creativecommons.org/licenses/by-nc-nd/4.0/
Type	journal article
File Information	NIMPR B347 26-38.pdf

Hokkaido University Collection of Scholarly and Academic Papers : HUSCAP

Reexamination of cross sections of the ^{100}Mo(p,2n)^{99m}Tc reaction

S. Takács[a,1], A. Hermanne[b], F. Ditrói[a], F. Tárkányi[a], M. Aikawa[c]

[a] Institute for Nuclear Research, Hungarian Academy of Sciences, 4026 Debrecen, Hungary
[b] Cyclotron Laboratory, Vrije Universiteit Brussel, Brussels 1090, Belgium
[c] Faculty of Science, Hokkaido University, Sapporo 060-0810, Japan

Abstract

The nuclear medicine community has been expressing concerns world wide regarding shortages of ^{99m}Tc supply based on fission production of ^{99}Mo from highly enriched uranium (HEU) to prepare ^{99}Mo/^{99m}Tc generators. As an alternative to reactor produced ^{99}Mo/^{99m}Tc generator technology, the direct production of ^{99m}Tc on accelerators is considered. There are a number of methods of using accelerators to produce ^{99m}Tc and/or ^{99}Mo. Direct production of ^{99m}Tc on highly enriched ^{100}Mo target using cyclotrons is interesting for energies up to 20 MeV, so as to minimize the impurities from additional open reaction channels. To estimate the quality of the accelerator produced ^{99m}Tc all the possible reaction routes should be mapped which could be potentially involved in this technology. However, a well defined excitation function for the ^{100}Mo(p,2n)^{99m}Tc primary reaction is needed, in order to achieve acceptable good results in assessing the quality of the accelerator-produced ^{99m}Tc by theoretical calculations. Most of the available experimental cross section data series for the ^{100}Mo(p,2n)^{99m}Tc reaction have the same general shape while their amplitudes are different. A large difference more than a factor of two may, indeed, be observed between the lowest and the highest datasets values.
The aim of this study was therefore to get a new evaluation for the ^{100}Mo(p,2n)^{99m}Tc cross section, through three independent experiments, aiming at a more confident estimation about the amplitude of the excitation function.

Keywords: ^{99m}Tc, ^{99}Mo, cross section, cyclotron

1. Introduction

Diagnostic imaging techniques in nuclear medicine using ^{99m}Tc radionuclide account for more than 70% of all procedures. Unfortunately, reliable supply of ^{99m}Tc might result in a future risk due to the aging of the few authorized ^{99}Mo-producing research reactors and processing facilities. Their scheduled shutdown and failures, as already experienced in the recent past, might bring to a global supply shortage of ^{99}Mo. Efforts and studies are going on the alternative production routes under investigation on ^{99}Mo and ^{99m}Tc all over the world [1, 2, 3, 4]. Direct production of ^{99m}Tc with accelerators is one of the proposed alternative production route utilizing the ^{100}Mo(p,2n)^{99m}Tc reaction on highly ^{100}Mo-enriched target material [5]. Recently the International Atomic Energy Agency (IAEA) has launched a Coordinated Research Project

[1] Corresponding author: S. Takács, email: stakacs@atomki.hu

(CRP) on alternative direct production of ^{99m}Tc using dedicated cyclotrons [6]. The eventual production of ^{99m}Tc may likely not be based on low current medical cyclotrons.

A study on this reaction by measuring the excitation function versus the bombarding proton energy was already carried out rather early by Beaver et al. [7]. Since then, several other studies were published on the ^{100}Mo(p,2n)^{99m}Tc excitation function with conflicting results regarding the amplitude of the reported data. Errors were discovered for certain experiments and data were corrected. For example, results provided by Levkovskij should be normalized down by 18% due to the used value of the monitor reaction [8]. The early work of Lagunas-Solar et al. 1991, has an energy scale problem and misinterpretation of the contribution of ^{90}Nb [9]. The dataset published in 1999 by the same research group have a proper energy scale. But the data points are scattered very much and the excitation function shows resonance-like peaks [10] which is not the case for a (p,2n) reaction. Scholten et al. reported an excitation function in their work in 1999 [11] with one of the lowest amplitude. Our group has reported data with relative low amplitude in 2003 [12]. Meanwhile new evaluated values regarding the decay data of ^{99}Mo and ^{99m}Tc radionuclides were published in 2004 [24], which partly could explain the reported low cross section values of the ^{100}Mo(p,2n)^{99m}Tc reaction. Additional experimental works and data have been reported with large difference regarding the amplitude of the reaction during the past 10 years by [13, 14, 15, 16, 17, 18, 19, 20, 21, 22] using both natural Mo and enriched ^{100}Mo targets. The available cross section database of the ^{100}Mo(p,2n)^{99m}Tc reaction contains several datasets now, but a critical evaluation of the experimental data is urgently needed. In Fig. 1 we have collected the published results which clearly show that the quality of this database requires significant improvements. Qaim et al. gave a comprehensive analysis of the available data in 2014 [23] introducing an effective cross section and using a theoretical approach. However, when datasets are different from each other in such an extent, there should be some among them which are basically not correct. In a first step of the data analyses, these erroneous datasets should be identified and corrected whenever possible otherwise they should be discarded. The reduced database thus obtained is more suitable for preparing recommended values for the reaction. Moreover, in this work we performed new experiments using the stacked target foil technique, activation method and gamma-spectrometry for measuring cross sections of the ^{100}Mo(p,2n)^{99m}Tc reaction in well controlled conditions, in order to be able to provide a limit for the amplitude of the excitation function.

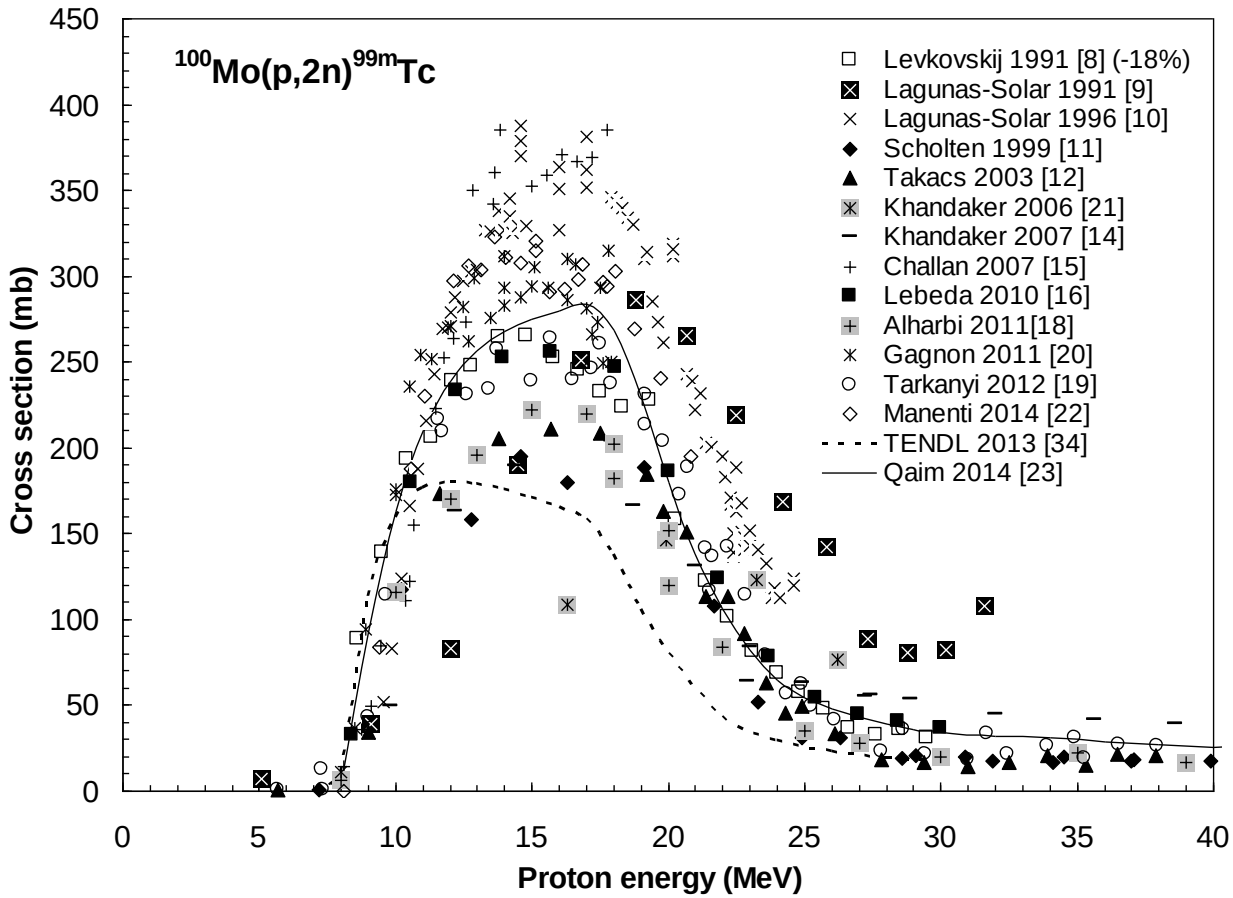

Figure 1. Available experimental cross section data and theoretical calculations for the ^{100}Mo(p,2n)^{99m}Tc reaction.

2. Analysis of possible error sources

2.1. Possible errors among experimental cross sections

Analyzing data in Fig. 1 it may be argued that two of them [9, 21] are markedly different from the others and show a shifted energy scale. Removing those two datasets the remaining ones were normalized, by simply rescaling each excitation function with different subjective scale-factor until a reasonably good agreement were found (see Fig. 2). After this linear rescaling of the amplitudes looking at the data plotted in Fig. 2, two main features may be inferred:

1) The agreement among the datasets is much better after rescaling, indicating that some of the dataset may contain different unknown systematic errors.
2) Data points above 15 MeV appears to be more scattered. This behaviour can be explained by considering that ^{99}Mo is always produced and the direct and indirect decay contributions of ^{99}Mo to the E_γ=140.5 keV (see later) need to be separated which could result in more scattered cross section data. The practical production threshold for ^{99}Mo is just above 10 MeV. Although some of the data were measured by using ^{100}Mo enriched target with different enrichment levels [8, 11, 20, 22] the ratio of the ^{99m}Tc and ^{99}Mo produced however does not depend on the enrichment level since both radioisotopes are

produced from the same ^{100}Mo target atoms. Another possible effect which may accounted for is the ^{90}Nb production. Above 15 MeV production of ^{90}Nb is indeed energetically possible on Mo targets with natural isotopic composition, because of ^{94}Mo and ^{92}Mo isotopes contribution, although its practical thereshold is above 20 MeV. Its decay contributes by emission of E_γ=141 keV gamma-photons to the E_γ=140.5 keV gamma peak of the ^{99m}Tc in the spectra which cannot be resolved by the detector. Separation of the ^{90}Nb contribution produces additional scatter of the data points.

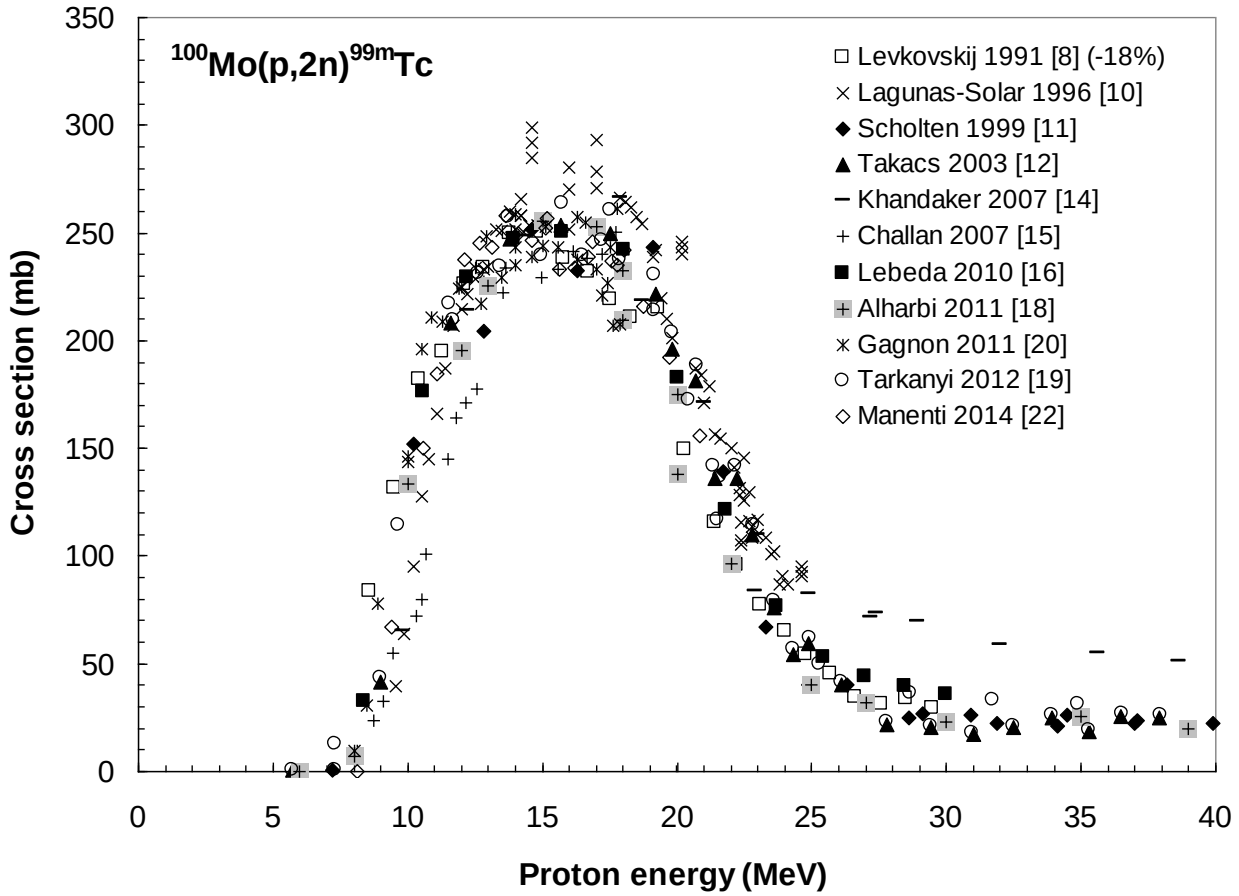

Figure 2. The agreement is shown to appear much better among the selected datasets (see text) after a subjective rescaling of their amplitude, indicating that the experimental data may include different amount of unknown systematic errors.

There are several error sources that could contribute to those differences among the reported datasets:

1) Beam current
2) Target thickness
3) Detector efficiency
4) Nuclear decay data
5) Problematic peak analysis
6) Latent cooling time error

2.1.1. The beam current and target thickness

Errors on beam current and target thickness measurements could influence in a similar way the activation cross section measured for all reaction products in an activated Mo target foil. In those cases where there is discrepancy among the amplitudes of the reported excitation functions for the ^{99m}Tc reaction but a good agreement can be found for the activation cross section of the other Tc products, the possible systematic error contributions in the beam current and target thickness measurement is minimal, therefore it may not be considered as an explanation to the large observed deviation of the ^{99m}Tc cross section. Any possible correction in the deduced cross sections, due to systematic errors in beam current and target thickness measurement, can be made in most cases only by the authors, who can check and modify if necessary the used beam intensity and target thickness values. Correction may be easily done as it requires only a simple re-scaling of data, according to the rate of the discovered systematic error. In general a (p,2n) excitation function is a smooth curve having one maximum and without resonances or resonance-like peaks. However, some of the published datasets are scattered and have resonance-like feature [10, 15, 19, 20, 22]. When determining excitation functions by irradiating several single foils or stacks of foils with overlapping energy regions and/or with different foil thicknesses may result that the derived cross section points are scattered due to systematic errors in beam current and/or target thickness measurements indicating problems with the used measuring technique and/or target preparation.

2.1.2. The detector efficiency

The detector efficiency is one of the possible sources of the large deviations among the available datasets. The E_γ=140.5 keV gamma-line of the ^{99m}Tc is in the energy region where the geometry dependent detector efficiency curve may contain the largest systematic error. The E_γ=140.5 keV energy is laying in the bended region of the detector efficiency curve, using log-log scale, which is generally approximated with different type of polynomial equations. In case when the shape of the efficiency curve is not well calculated a significant systematic error can be introduced to the measured ^{99m}Tc cross section data. However, correction of a systematic error in detector efficiency can be made only by the authors who can check and modify, if necessary, the used detector efficiency curve. The correction means linear rescaling of the cross section data. Cross sections having similar values determined from an acquired spectrum by using a low and a high energy gamma-lines of the investigated radionuclide indicate a proper shape of the used detector efficiency curve.

2.1.3. Decay data

The nuclear decay data is one certain source of the deviations. Due to the decay scheme of ^{99}Mo and ^{99m}Tc the use of the proper decay branching ratios and gamma intensities is essential. The actual values of these data can vary for different evaluations. The early data are slightly different from the recent ones. The simplified decay scheme of ^{99}Mo and ^{99m}Tc is shown in Fig. 3. ^{99}Mo decays to ^{99g}Tc in 12.4% while 87.6% of the decay populates the higher laying isomer state ^{99m}Tc (E=142 keV, $T_{1/2}$=6h). About 5.1% of the decay of ^{99}Mo contributes to the population of the E=140.5 keV energy level of ^{99}Tc resulting in emission of direct or prompt E_γ=140.5 keV gamma photons. The longer lived isomeric state, ^{99m}Tc decays almost 100% (IT=99.9963%,

β^-=0.0037%) to the E_γ=140.5 keV energy level and then to the ground state of ^{99}Tc by emission of an E_γ=140.5 keV gamma photon.
The gamma intensities used in this work are taken from the evaluation presented in 2004 by Bé et al. [24] and are collected in table 1. Due to the simultaneous decay of ^{99}Mo and ^{99m}Tc present in the irradiated Mo foil it is "easy" to introduce systematic error during data evaluation, especially when different approximations are used in data analysis and cross section calculations. Knowing the decay data used by the authors in their data evaluation in principle data can be corrected. Due to the lack of the necessary input data (such as cooling time, acquisition time etc.), it is however quite hard (or impossible) by an evaluator do, in practise, the proper corrections. Only authors can do that.

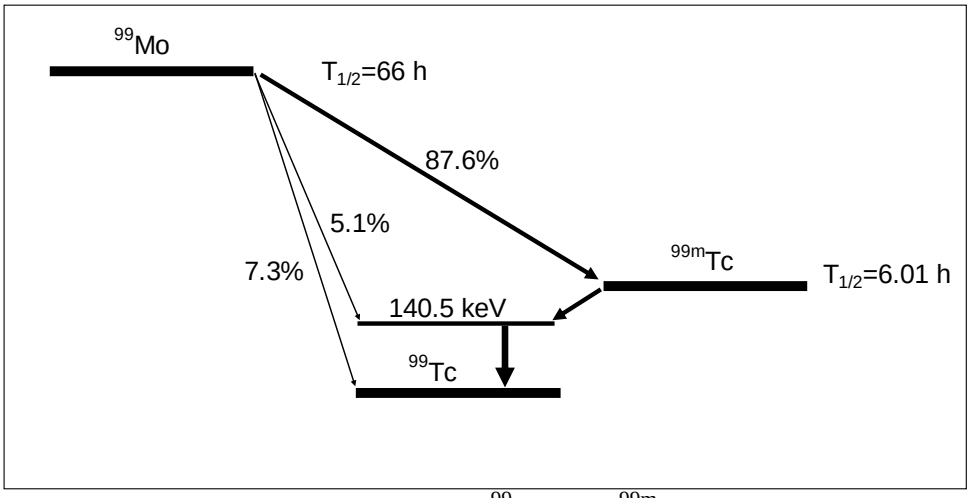

Figure 3. Simplified decay scheme of ^{99}Mo and ^{99m}Tc.

Table 1. Intensities of the E_γ=140.5keV gamma photons emitted from different sources used in this work [24].

Intensity of the E_γ=140.5 keV gamma-line from different sources	I_γ (%)
Prompt gamma intensity of the decaying ^{99}Mo	4.72
In equilibrium of the decaying ^{99}Mo and ^{99m}Tc	89.6
Decay of pure ^{99m}Tc (no decaying ^{99}Mo is present):	88.5

2.1.4. Gamma-peak analysis for ^{99}Mo and ^{99m}Tc

Production of ^{99}Mo radionuclide starts promptly when irradiation begins and ends at the end of bombardment (EOB) when irradiating a Mo foil with a proton beam having energy higher than 8 MeV. The radionuclide ^{99m}Tc is instead produced both directly and by decaying of the parent isotope ^{99}Mo during the irradiation. At the irradiation stop no more ^{99}Mo is thus yielded, but production of ^{99m}Tc still continues by ^{99}Mo decay after EOB, during both cooling time and measuring time, as well. After a certain cooling time, the first gamma spectrum measurement of the irradiated Mo foil can be started and information in the E_γ=140.5 keV gamma-peak may be gathered during the applied acquiring time. This peak may contain information on the production of both radionuclides, information on the cross section of direct ^{99m}Tc production because of the

direct Mo(p,2n) reaction route, as well as the cumulative cross section for the ^{99}Mo production (including the ^{100}Mo(p,pn), ^{100}Mo(p,d) and ^{100}Mo(p,2p)^{99}Nb→^{99}Mo processes). Different corrections to the peak area should be provided, when calculating the cross section, depending on the bombarding proton energy, the applied cooling time and different gamma intensities of the E_γ=140.5keV gamma photons. Use of different approximations or inappropriate corrections for the different contributions to the measured peak area might account for most of the systematic errors which may result in those large deviations among the different datasets. Moreover, the possible interference with the E_γ=141keV gamma line of the decaying ^{90}Nb and the cumulative production of ^{99}Mo by decay of ^{99}Nb at bombarding proton energies higher than 15 MeV should be taken into account. Correction of a systematic error due to use of erroneous decay parameters and/or improper data analysis can be made only by the authors who need to have every parameters of the experiment. The correction is not linear regarding the half-lives and timing information (irradiation, cooling and measuring time). The rescaling of the result for corrected gamma intensities is more complex due to the different contributing sources to the E_γ=140.5keV gamma-peak.

2.1.5. Latent cooling time error

It is a common rule that that experiments are partly conducted and/or controlled by computers. Usually different phase of an experiment is controlled by different computer (irradiation, data acquisition). In case the clock of the controlling computers are not synchronised it could result in use of erroneous cooling time. Error in cooling time influences the deduced cross section data especially for a radionuclide with short half-life. Use of the proper cooling time in case of ^{99m}Tc is even more important due to its production after EOB by decay of ^{99}Mo.

2.2. Cross section measurement

In this work, the ^{100}Mo(p,2n)^{99m}Tc reaction cross section was repeatedly measured, in three independent experiments, aiming at a more confident estimation about the amplitude of the excitation function. In the cross section calculations the following approximations were applied:

- Constant beam current during the whole irradiation time
- Thin target foil, in which the energy degradation of the bombarding particles can be approximated by a linear function
- The cross section within the thin irradiated foil can be approximated by a linear function

then the deduced cross section can be assigned to the mid-energy point of the target foil (the simple average of the incoming and outgoing energy of the bombarding particles).

2.2.1. Data processing for determining the activation cross section of ^{99}Mo and ^{99m}Tc

Regarding a single peak in a gamma-spectrum, the peak area (i.e. the total number of counts in the peak) once removed the background, is generally proportional with the number of decays occurring in the sample during the applied acquisition time. However, in the gamma-spectrum of an activated Mo foil the E_γ=140.5keV gamma peak can have four different origins, these are:

- Decay of direct produced ^{99m}Tc, (Eq.1)
- Decay of ^{99m}Tc produced during irradiation exclusively by decay of ^{99}Mo, (Eq.2)
- Decay of ^{99m}Tc produced after EOB by decay of ^{99}Mo, (Eq.3)

- Prompt gamma radiation that follows the decay of ^{99}Mo, (Eq.4)

The corresponding contributions to the total peak area T_γ acquired during a t_m measuring time after a t_b irradiation and t_c cooling time for a given Mo target foil can be described by the following four equations for the above four components, respectively.

$$T_\gamma(direct)_D = \varepsilon_d \varepsilon_{\gamma_2} \varepsilon_t N_t N_b \sigma_2 \left(1 - e^{-\lambda_2 t_b}\right) \frac{1}{\lambda_2} e^{-\lambda_2 t_c} \left(1 - e^{-\lambda_2 t_m}\right) \quad (1)$$

$$T_\gamma(decay)_x = \varepsilon_d \varepsilon_{\gamma_2} \varepsilon_t \frac{f N_t N_b \sigma_1}{(\lambda_1 - \lambda_2)} \left[\lambda_1 \left(1 - e^{-\lambda_2 t_b}\right) - \lambda_2 \left(1 - e^{-\lambda_1 t_b}\right)\right] \frac{1}{\lambda_2} e^{-\lambda_2 t_c} \left(1 - e^{-\lambda_2 t_m}\right) \quad (2)$$

$$T_\gamma(decay)_y = \varepsilon_d \varepsilon_{\gamma_2} \varepsilon_t \frac{f N_t N_b \sigma_1}{(\lambda_1 - \lambda_2)} \left(1 - e^{-\lambda_1 t_b}\right) \left[e^{-\lambda_2 t_c} \left(1 - e^{-\lambda_2 t_m}\right) - \frac{\lambda_2}{\lambda_1} e^{-\lambda_1 t_c} \left(1 - e^{-\lambda_1 t_m}\right)\right] \quad (3)$$

$$T_\gamma(direct)_M = \varepsilon_d \varepsilon_{\gamma_1} \varepsilon_t N_t N_b \sigma_1 \left(1 - e^{-\lambda_1 t_b}\right) \frac{1}{\lambda_1} e^{-\lambda_1 t_c} \left(1 - e^{-\lambda_1 t_m}\right) \quad (4)$$

Where

N_t surface density of target atoms, [atom/cm^2]
N_b number of bombarding particles per unit time, [proton/sec]
σ_i activation cross sections, [cm^2]
f decay branching ratio of ^{99}Mo to ^{99m}Tc
ε_d detector efficiency
ε_γ corresponding gamma intensity
ε_t dead time correction
λ_i decay constant, [1/sec]
t_b bombarding time, [sec]
t_c cooling time, [sec]
t_m acquisition time, [sec]
i the *i=1* index refers to the ^{99}Mo parent radionuclide, *i=2* is referred to the ^{99m}Tc daughter radionuclide instead.

Please note that only Eq. 1 contains information about the direct production cross section of ^{99m}Tc. Therefore in the peak analysis we need to remove the contributions of the other three components. In Fig. 4 the contributions of the four components to the measured total peak area is shown on a relative scale as function of cooling time for a given proton energy and irradiation time. The magnitudes of the four contributions also depend on the length of the irradiation time and the proton energy since the cross sections are energy dependent.

Determining the direct production cross section of ^{99m}Tc a short irradiation with an intense proton beam, followed by a short cooling time (preferably both the t_b and t_c should be less than one tenth of the half life of ^{99m}Tc) can provide a good approximation of Eq. 1 and can be used to determine the cross section for the ^{100}Mo(p,2n)^{99m}Tc reaction. However, when the above criterions are not fully met, without appropriate correction of the measured peak area, the excitation function thus estimated will definitely be larger than the real value. In this work the above four analytical equations were used and no approximation method was applied. As it can be seen in Fig. 4 the contribution of the direct-produced ^{99m}Tc drops down steadily according to its half life

($T_{1/2}$=6.01h). After a long cooling time, the collected counts will no longer contain information about the cross section of the ^{100}Mo(p,2n)^{99m}Tc reaction.
The spectra measured after the direct produced ^{99m}Tc component has lowered, still can have a strong E_γ=140.5keV peak that can be used to determine the cross section of the ^{100}Mo(p,x)^{99}Mo process by using the gamma intensity (I_γ=89.6%) valid for the equilibrium stage.
In a routine spectrum analysis it is easy to make mistakes by taking gamma intensities automatically from data tables. Checking the relevant decay radiation table of ^{99}Mo in NuDat-2.6 [25] no E_γ=140.5keV gamma line is listed in the table. In the work of the latest compilation by Bé et al. 2004 [24] the E_γ=140.5keV gamma line is included in the table but no indication is given there that the presented gamma intensity is valid only for the equilibrium stage between the two decaying radionuclides ^{99}Mo and ^{99m}Tc. This is mentioned four pages above in their report. Without paying enough attention an automatic use of these two tables could lead to erroneous results.
In this work the nuclear decay data of the investigated radionuclides were taken from the on-line database NuDat-2.6 [25] and [26]. Except for decay data of ^{99}Mo and ^{99m}Tc, which were taken from the latest compilation work by Bé et al. [24] and are summarized in Table 2.

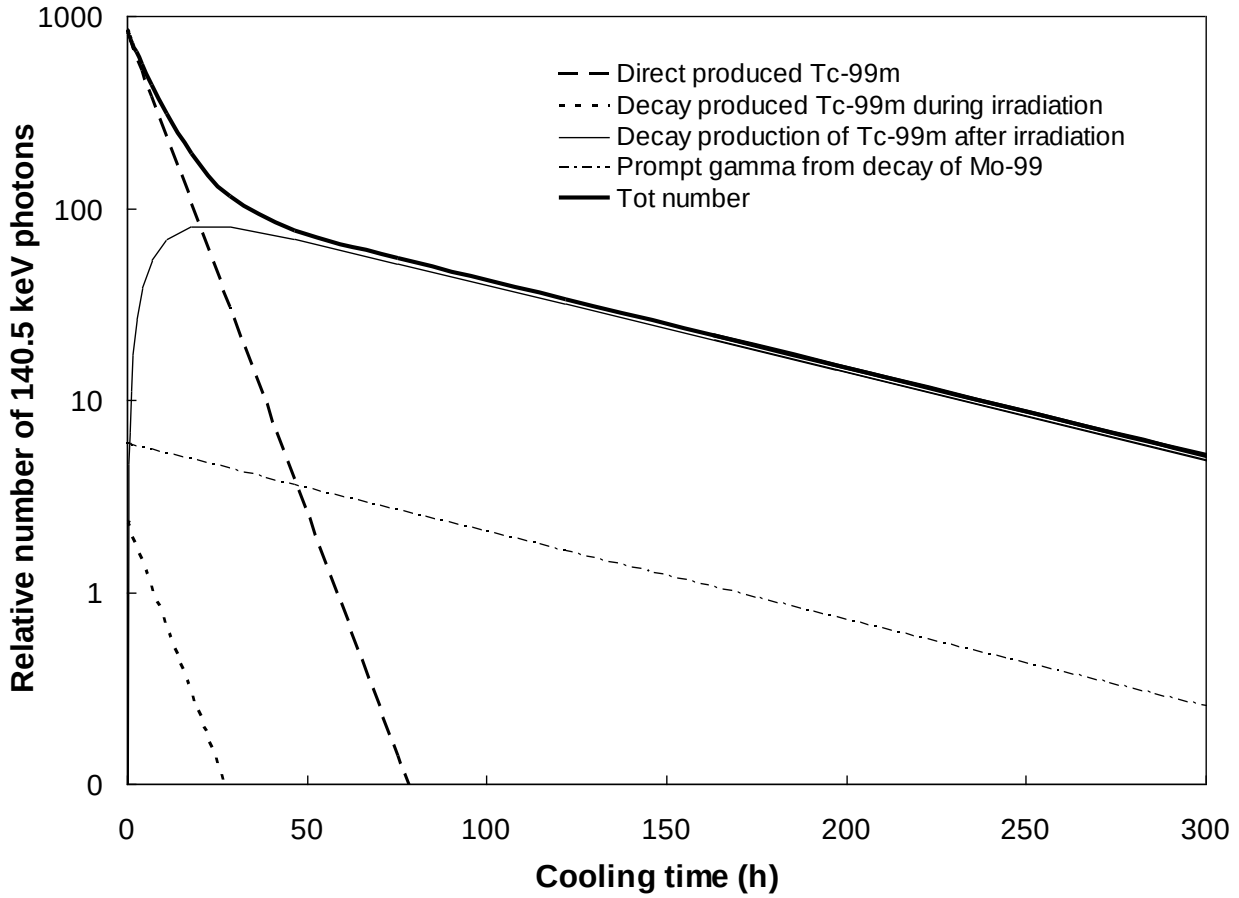

Figure 4. Relative contributions to the total peak area of the E_γ=140.5keV gamma line of the four components as function of the cooling time. (EOB=0).

Table 2. Nuclear decay data used in this work taken from [25], and [26]. Data with * are from [24].

	Half life	Decay mode	E_γ keV	I_γ %	Contributing reactions	Q-value MeV [26]	Threshold MeV [26]
^{99}Mo	65.9496* h	β^-, 100%	140.5	4.72*	^{100}Mo(p,pn)	-8.29	8.38
			181.1	6.01*	^{100}Mo(p,d)	-6.07	6.13
		^{99}Mo→^{99m}Tc	739.5	12.12*	^{99}Nb decay		
		87.6%*	140.5 (equilibrium)	89.6*			
^{99g}Nb	15 sec	β^-, 100%	137.7	81.0	^{100}Mo(p,2p)	-11.15	11.26
^{99m}Nb	2.6 min	β^-, 96.2% IT, 3.8%	97.8	6.7			
^{99g}Tc	2.14x10^{3}* year	β^-, 100%	89.5	6.5x10^{-4}	^{100}Mo(p,2n)	-7.72	7.79
^{99m}Tc	6.0082* h	IT, 99.9963% β^-, 0.0037%	140.5	88.5*			
^{90g}Nb	14.6 h	EC, 48.8%	141.18	66.8	^{94}Mo(p,αn)	-8.96	9.05
		β^+, 51.2%	1129.22	92.7	^{92}Mo(p,^{3}He)	-11.79	11.92
^{90m}Nb	18.8 sec	IT, 100%	122 (?)	(?)			
^{90}Mo	5.67 h	EC, 100%	122.37	64	^{92}Mo(p,t)	-14.30	14.45
			257.34	78			
^{48}V	15.9735 day	EC, 100%	983.5	99.98	^{48}Ti(p,n)	-4.78	4.90
			1312.1.	98.2	^{49}Ti(p,2n)	-12.94	13.21

* : Data are taken from [24].

The standard atomic weight (A_{Mo}=95.96(2)g) and the isotopic composition of molybdenum (^{92}Mo:14.525(15)%, ^{94}Mo:9.1514(74)%, ^{95}Mo:15.8375(98)%, ^{96}Mo:16.672(19)%, ^{97}Mo:9.5991(73)%, ^{98}Mo:24.391(18)% and ^{100}Mo:9.824(50)%) were taken from a IUPAC Technical Report 2009 [27] and were used in the calculations.

3. Experimental

3.1 Target preparation

The stacked foil technique, proton activation and high resolution gamma-spectrometry methods were used for measuring the cross sections of the ^{100}Mo(p,2n)^{99m}Tc reaction using thin molybdenum foils in metallic form with natural isotopic composition as target. Two stacks were irradiated at 16 MeV and 36.4 MeV incident proton energies at Atomki, Debrecen and VUB, Brussels, respectively. Each target foils was 10x10 mm rectangular cut out from a larger sheet which was weighted on a microbalance and the surface was measured precisely to be able to determine an average thickness which was used in the data evaluation. The Mo foils were ordered by Goodfellow, UK (nominal thickness 12μm, measured average thickness 11.98 μm, chemical purity: 99.9%). The stacked target in Atomki was assembled from 14 groups of Mo-Mo-Ti foils in sequence and additional 7 Ti foils were added at the end of the stack. Two molybdenum foils

followed each other in each group in order to check the strength of the possible recoil effect. Due to the used thin foils and the low variation of the expected recoil intensity as function of bombarding energy, we supposed that the amount of the recoiled reaction products is approximately the same for both of the Mo foils in sequence. Therefore no recoil correction is needed for the second Mo foil in each group. The first Mo foil of a group also served as a catcher foil for the reaction products recoiled from the previous Ti foil. The Ti foils were (nominal thickness 12μm, measured average thickness 12.05 μm, chemical purity: 99.9%, Goodfellow, UK) used to monitor the beam parameters and also served as energy degrader and catcher foil for the possible recoiled reaction products leaving the Mo foils in front. An additional aim of the experiment was to provide new cross section data points close to the threshold energy of the ^{nat}Ti(p,x)^{48}V reaction. Therefore additional 7 Ti foils were placed after the 14 Mo-Mo-Ti groups in the low energy section of the stack. The target foils were assembled in a simple Faraday-cup type target holder. The stack at VUB was assembled by using Mo, Sm, Ti and Al foils. The Mo and Ti foils were the same type as in the Atomki experiment. The samarium foils were ordered by Goodfellow, UK (nominal thickness 25μm, measured average thickness 26.8 μm, chemical purity: 99.9%) and were used as another target material. Al foils for energy degradation, ordered by Goodfellow, UK (nominal thickness 100μm, measured average thickness 98.0μm, chemical purity: 99.9%). The stack consisted of 18 groups of Ti-Sm-Ti-Al-Mo-Al foils.

3.2 Irradiation and activity measurements

The irradiation was done at an external beam line of the MGC20E cyclotron of Atomki, Debrecen and at the CGR-560 cyclotron of VUB in a specially designed Faraday-cup-like, air cooled vacuum chamber equipped with a water cooled long collimator (5 mm in diameter), assuring that all incoming charged particles hit the target foils. The schematic drawing of the irradiation setup is shown on Fig 5.

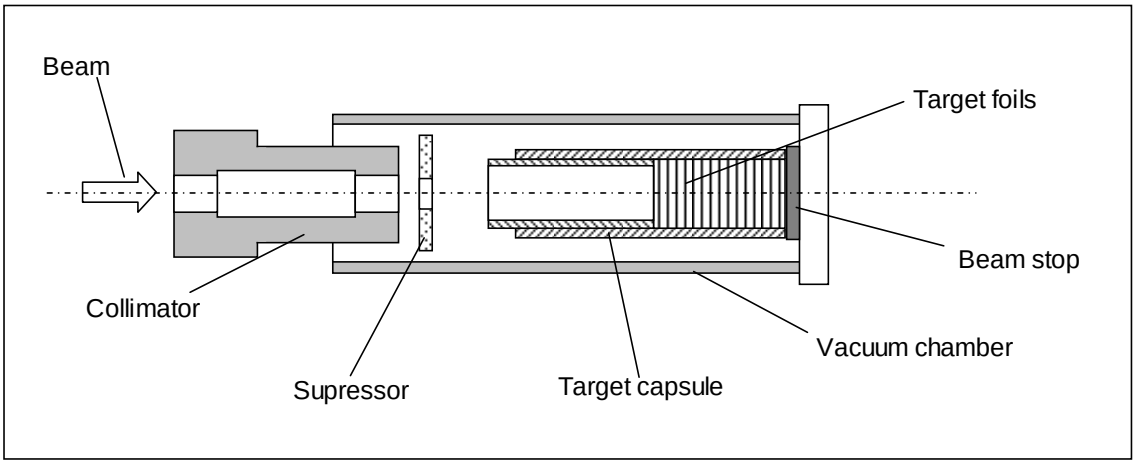

Figure 5. Schematic drawing of the irradiation setup

An electron suppressor was used in the irradiation chamber on which -300V electric potential was applied in order to prevent the electrons kicked out from the target surface by the proton beam from escaping the irradiation chamber in the Atomki experiment. No electron suppressor was applied in the VUB experiment, therefore the ^{nat}Ti(p,x)^{48}V monitor reactions was used for determining the beam intensity. The initial bombarding proton beam energy was set to

16 MeV, the beam intensity 116nA and the irradiation time 1.8h at the Atomki cyclotron. The energy of the proton beam was 36.4 MeV, the beam intensity 103nA and the irradiation time 1h at VUB cyclotron, instead. The initial beam energy were determined at both site using the settings of the cyclotron calibrated earlier by time of flight method and resonance nuclear reactions and was checked by the $^{nat}Ti(p,x)^{48}V$ monitor reaction. The beam current was kept constant during irradiation. A digital charge integrator was used to record the amount of collected charge at both sites. At the Atomki experiment it served as the accurate determination of the total number of incident particles during irradiation.
After irradiation a short, less than 1 hour cooling period was allowed before the foils were separated from the stack and individually enclosed in a small marked plastic bag for gamma spectroscopic measurement. The activity of the produced radionuclides in each target and monitor foils was assessed without chemical separation using a high resolution HPGe gamma-ray spectrometer. A high purity germanium detector manufactured by Canberra (p-type at Atomki and n-type at VUB) were used. The detector at Atomki was coupled to a Tenelec and Canberra acquisition and Nucleus analyzing system to acquire the gamma-spectra. At VUB Canberra electronics and Genie2000 analyzing system was used to record spectra. Minimum 3 series of measurements were performed for each Mo target. In a given series foils were measured at the same detector-sample distance. The first measurement at Atomki started at 0.9 hour cooling time after the end of bombardment (EOB) and each measurement lasted about 10 minutes. For the second series of the measurement the cooling time was between 50 and 270 hours after EOB while the measuring times were between 6 and 24 hours. Spectra in the third series of measurement were recorded after 470 and 900 hour of cooling time applying at least 7 hours of acquisition time. The first series of measurement at VUB started after a 3h cooling time and each measurement lasted about 10 minutes. For the second series of the measurements the cooling time was between 50 and 75 hours after EOB while the measuring times were between 0.6 and 10 hours. Spectra in the third series of measurement were recorded after minimum 500 hour of cooling time applying at least 2 hours of acquisition time. Measurements were done with different sample–detector distances. The detector sample distance was set between 50 and 5 cm, keeping the pileup effect and dead time of the electronics low, but every measurement in a given series was done at the same distance. Typical dead time varied from <3% for the first series of measurements to ≤ 0.1% for the late measurements. Each Ti monitor foil was measured about one month after EOB, allowing decay of the co-produced small amount but interfering ^{48}Sc isotope.
The geometry dependent efficiencies of the detectors were determined in those fixed positions which were used in the data acquisition. Low reference activity ^{57}Co, ^{133}Ba, ^{152}Eu, and ^{241}Am calibrated standard gamma-sources with max. 1.5% uncertainty were used to determine the efficiency of the detector in the used positions. The net peak area of the photo peak in the spectra corresponding to the given gamma-ray was calculated using the peak fitting algorithm included in the GENIE acquisition software and FORGAMMA [28] interactive peak analysis code.

3.3. Cross section calculation and uncertainties

Cross-sections were calculated according to the general activation formula (Eq. 1) using corrected peak area when it was necessary as in the case of ^{99m}Tc. The uncertainty of each cross-section data point is given by combining the individual error components in quadrature: target thickness 1%, beam current 3%, peak area including fitting uncertainty and separation of contributions 2%-10%, detector efficiency 3%, and decay parameters 3%. The overall uncertainty of the measured cross section points are 6-12%. The measured activation cross sections for ^{99}Mo

and ^{99m}Tc are normalized to 100% enrichment of ^{100}Mo since they are produced practically only on ^{100}Mo isotope. The uncertainty of the initial bombarding proton energy was ±0.25MeV and this value was assigned to the first Mo foil in the stack. The uncertainty of the energies assigned to the measured cross section points increased gradually with penetration of the beam into the target due to straggling effect and uncertainty of the foil thicknesses. The uncertainty of the energy in the last Mo foil reaches ±0.45 MeV and ±1.56MeV for the experiment at Atomki and at VUB, respectively.

4. Data evaluation

4.1. The ^{nat}Ti(p,x)^{48}V monitor reaction

The energy degradation of the bombarding proton beam in the stacked target was calculated by the STACK computer code based on energy loss calculation using the polynomial approximation method of Andersen and Ziegler [29]. The mid energy point of each layer in the stack defines the energy scale of the deduced excitation functions. The Ti monitor foils were measured about one month after EOB, allowing decay of the small amount of the co-produced interfering ^{48}Sc isotope. Both the 983 keV and the 1312 keV gamma lines were used in the data analysis. The cross section of the ^{nat}Ti(p,x)^{48}V monitor reaction was determined according to the basic activation equation using the deduced peak areas for both of the strong gamma-lines and the initial parameters of the experiment, by applying the beam intensity deduced from charge integration. The two gamma lines provided almost identical cross section values for each Ti foil (with 1.3% difference in average) drawing a smooth excitation function as function of bombarding proton energy. Each Mo target foil, followed the Ti foils in the stack of the Atomki experiment, was analysed for the two gamma lines of ^{48}V to determine the recoil correction factor. A correction of about 1.6% is needed to apply in case of the Ti foil in the stack having about 16MeV bombarding proton energy. This correction is gradually decreasing as the penetrating proton beam loosing its energy. The relative recoil correction factor in percentage is presented in Fig. 6 as function of the proton energy below 16 MeV.

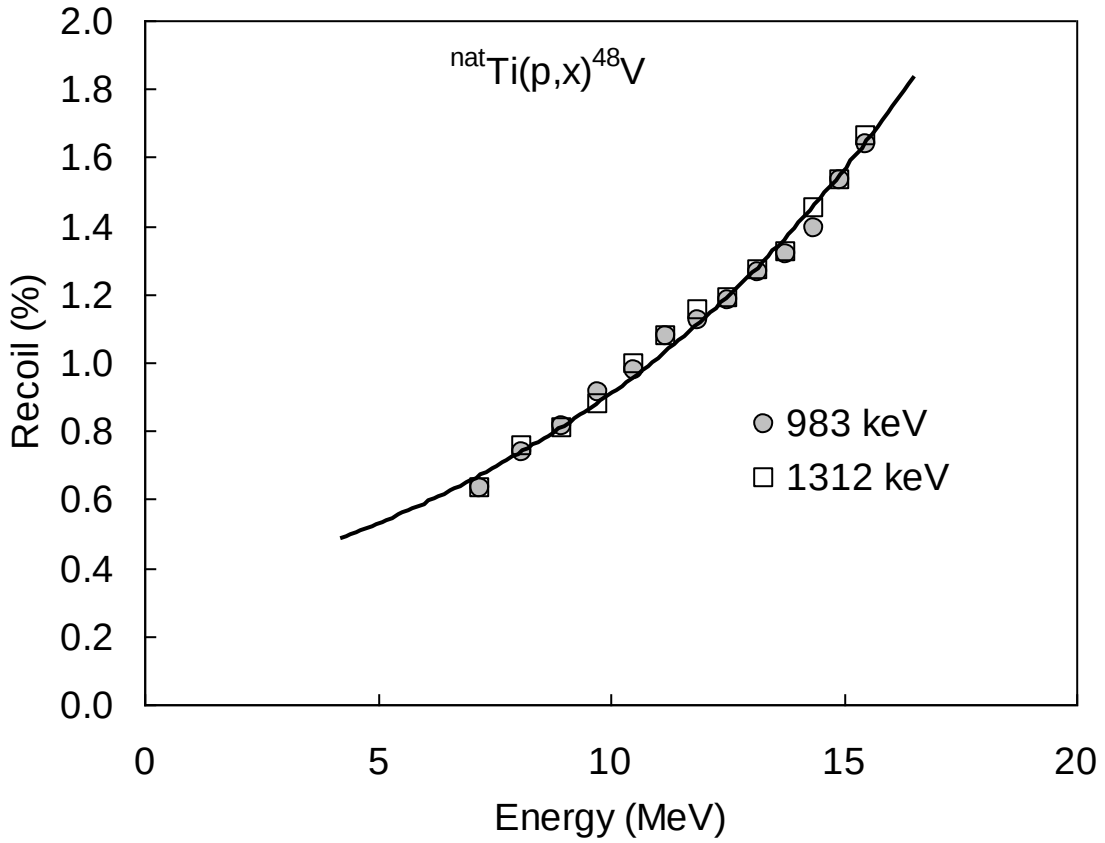

Figure 6. The relative amount of recoiled ^{48}V radionuclides is shown as a function of the bombarding proton energy. The solid line is a polynomial fit.

After correction of the recoil contribution an almost perfect agreement was found for the re-measured cross sections of the ^{nat}Ti(p,x)^{48}V monitor reaction with the recommended values taken from IAEA – TECDOC 1211 [30]. Comparing the amplitude of the recommended curve and the excitation function re-measured at Atomki about 2.5% disagreement was found. Down scaling the initial beam intensity, deduced from the charge integration by 2.5%, a good agreement was established between the two curves. The E_p=16MeV initial proton energy provides a perfect agreement for the energy of the first Ti foil of the Atomki experiment and the corresponding recommended value, but the shape of the measured curve is somewhat more narrow (see Fig. 7). Reducing the initial E_p=16MeV proton energy by 100keV to E_p=15.9MeV and recalculating the energy scale would result in a better agreement regarding the overall shape of the two curves. But while that 100keV change resulted in a better agreement regarding the overall shape of the two curves it moved the last point below the threshold of the reaction and the first point has no such a good agreement any more. Therefore the initial E_p=16MeV bombarding energy was kept.

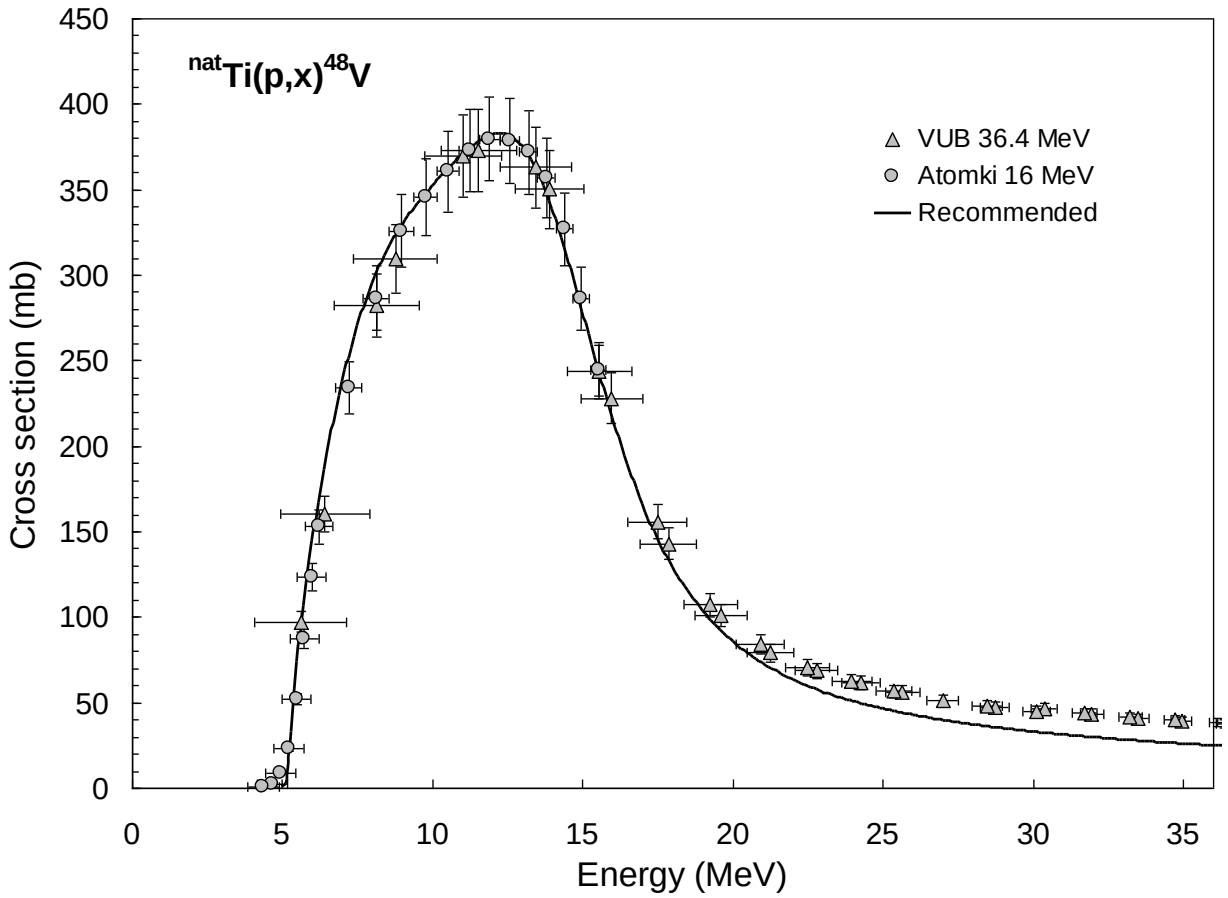

Figure 7. The re-measured $^{nat}Ti(p,x)^{48}V$ cross sections using the two intense gamma-lines in comparison with the recommended excitation function.

Please note that the 2.5% down scale correction of the absolute beam intensity increases the absolute height of the excitation function of the $^{100}Mo(p,2n)^{99m}Tc$ reaction by 2.5%. The excitation functions of the monitor reaction re-measured at Atomki and at VUB have perfect agreement in the overlapping energy region. The high energy tail of the deduced curve in the VUB experiment is systematically higher than the recommended one. We have always experienced this deviation which may indicate that a new evaluation of the monitor data may be required. Hopefully, this problem will be solved by the ongoing CRP of the IAEA to upgrade the monitor reaction data [31].

4.2. The $^{100}Mo(p,x)^{99}Mo$ reaction

The cumulative cross section of the $^{100}Mo(p,x)^{99}Mo$ process can be determined by using Mo targets with natural isotopic composition since no reactions on other stable isotope of molybdenum contributes. For determining the cumulative cross section of ^{99}Mo production (the sum of the $^{100}Mo(p,pn)^{99}Mo$, $^{100}Mo(p,d)^{99}Mo$ and $^{100}Mo(p,2p)^{99}Nb\rightarrow^{99}Mo$ reactions) the spectra measured after long cooling time were used. Applying at least 170 hours of cooling time it was ensured that no more ^{99m}Tc produced during irradiation was present in the target and the decaying ^{99}Mo and ^{99m}Tc were in equilibrium. In this condition the cross section for the ^{99}Mo production

can be determined on a standard way, by using the gamma intensity of the E_γ=140.5keV line valid for equilibrium stage. Spectra were measured for 7 to 24 hours and the collected net counts in the E_γ=140.5keV peak area was above 10.000 counts in each case. The cross sections were also calculated by using the two other independent gamma lines of ^{99}Mo (E_γ=181.1keV, I_γ=6.01% and E_γ=739.5keV, I_γ=12.12%) in the same spectra. The deduced cross section values calculated from the three different gamma peaks are in perfect agreement for each Mo foil. This good agreement between the cross section values calculated from the low energy E_γ=140.5keV and high energy E_γ=739.5keV gamma lines confirms that the shape of the detector efficiency curve is correct. The results of the two irradiations are included in Fig. 8 and Table 3 as one dataset.

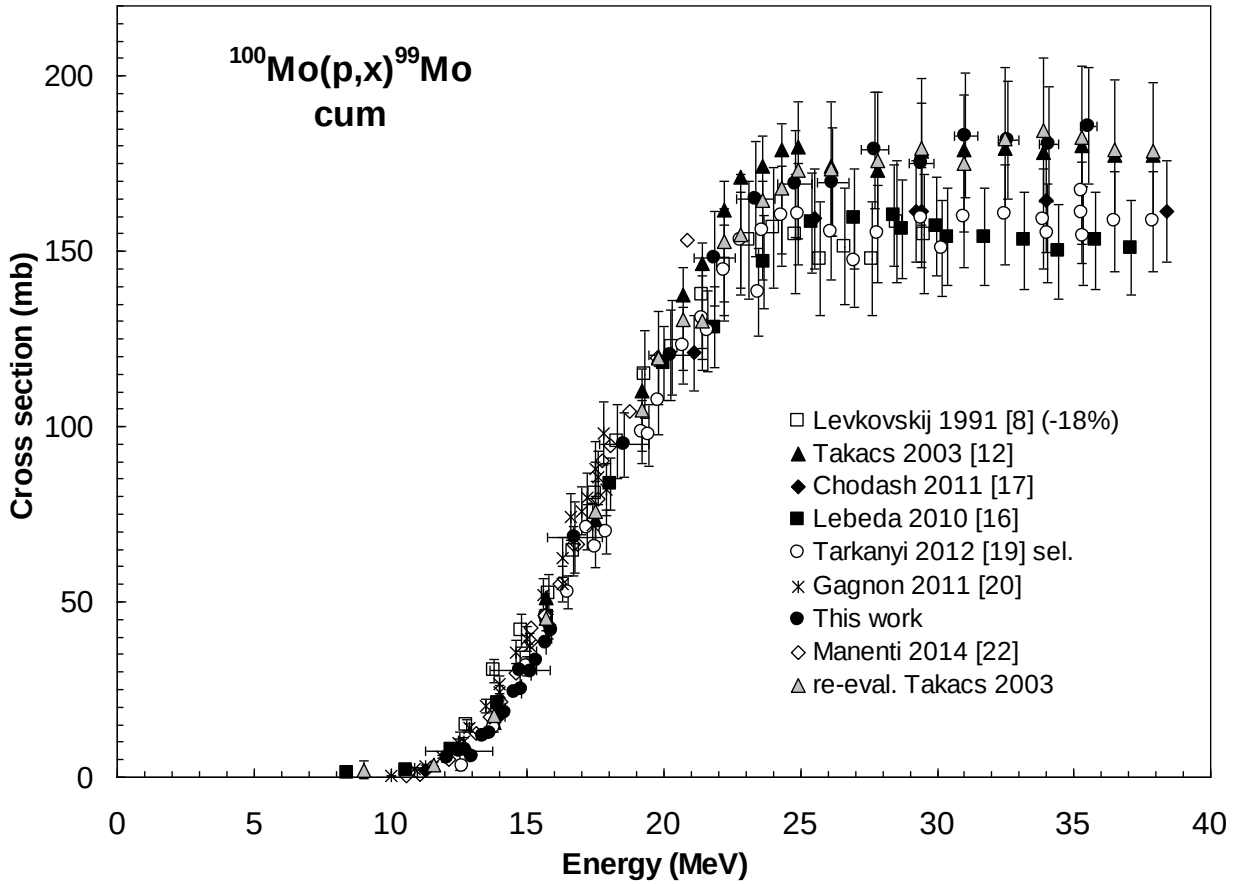

Figure 8. Excitation function of the ^{100}Mo(p,x)^{99}Mo process. Selected data sets, the newly measured points of this work and the re-evaluated results of [12] are presented. (From work of [19] only selected sub-data sets are included.)

Data of [9] and [11] were discarded due to the shape and too low amplitude of the excitation function. Some sub-data series from the work of Tarkanyi [19] were deselected as well. Moreover, one of our earlier experiments published in 2003 [12] were re-evaluated. The experiment was re-evaluated using the up to date decay [24] and monitor reaction data and an interactive spectrum analysis. To whole dataset was recalculated regarding the activation cross section of the ^{100}Mo(p,x)^{99}Mo and ^{100}Mo(p,2n)^{99m}Tc processes by applying an interactive peak analysis this time (not relying on the automated peak analysis software routine).

The re-evaluation of the 2003 experiment resulted in practically the same values for the ^{100}Mo(p,x)^{99}Mo process as were published before, except the small hump in the 20 and 25 MeV region which is not present there any more. In the 25 - 38 MeV energy region the original and the re-evaluated as well as the new experimental data are in good agreement. These datasets are the highest ones when comparing to all available datasets.

4.3. The ^{100}Mo(p,2n)^{99m}Tc reaction

The present experiments were performed with the aim to determine the amplitude of the excitation function of the ^{100}Mo(p,2n)^{99m}Tc reaction through some repeated, independent, experimental measurements, so as to provide additional experimental contributions and make an effort to clear the discrepancies that exist among the available data sets. The determination of the cross section for the ^{100}Mo(p,2n)^{99m}Tc reaction does not basically require a ^{100}Mo enriched material target. Indeed, only two reactions contribute to the direct production of ^{99m}Tc the ^{100}Mo(p,2n)^{99m}Tc main reaction and the ^{98}Mo(p,γ)^{99m}Tc reaction when using Mo target with natural isotopic composition. The (p,γ) reactions in general have low cross section. In this case the contribution from the (p,γ) reaction to the total amount of produced ^{99m}Tc is very small therefore can be ignored [11]. As it is shown in Fig. 1 the available data are very much different regarding their amplitude. There is a difference in the amplitude of the curves more than a factor of two. On the other hand the shapes of the curves are quite similar (see Fig. 2). Since there is no strong reference point it is difficult to judge how good the reported datasets are. In these new experiments we attempt to confirm the amplitude of the excitation function of the ^{100}Mo(p,2n)^{99m}Tc reaction by measuring cross sections in a well controlled manner. To determine the cross section of the ^{100}Mo(p,2n)^{99m}Tc reaction only the E_γ=140.5keV gamma-line is available in the spectra. After determining the peak area of the E_γ=140.5keV gamma-line in the spectra measured with short cooling times and by applying the above described corrections for the contributing sources (prompt radiation of the decaying ^{99}Mo, ^{99m}Tc produced by decay of ^{99}Mo during irradiation and ^{99m}Tc produced by decay of ^{99}Mo after irradiation) the cross sections were calculated. To calculate the corrections of the peak area measured for a given Mo foil the ^{99}Mo production cross section deduced from the same Mo foil was used. The resulting corrected net peak area was then used to determine the cross section of the ^{100}Mo(p,2n)^{99m}Tc reaction on the usual way for each irradiated Mo foil, by applying the gamma-intensity of 88.5%. In table 3 the applied cooling times and the relative intensities of the four contributing sources to the E_γ=140.5keV gamma-peak are given for the two irradiations.

Table 3. The applied cooling times and relative intensities of the four contributing sources of the E_γ=140.5keV gamma-peak area in 16 MeV and the 36.4 MeV irradiation.

Energy (MeV)	cooling time (h)	Direct prod. ^{99m}Tc (%)	Decay prod. ^{99m}Tc during irrad. (%)	Decay prod. ^{99m}Tc after irrad. (%)	Prompt rad. ^{99}Mo (%)

15.7	4.7	98.8	0.1	0.9	0.1
15.1	4.3	99.0	0.1	0.8	0.1
14.6	4.0	99.2	0.1	0.6	0.1
14.0	3.7	99.4	0.1	0.4	0.1
13.4	3.5	99.7	0.0	0.2	0.0
12.7	3.2	99.7	0.0	0.2	0.0
12.1	2.9	99.9	0.0	0.0	0.0
11.4	2.6	100.0	0.0	0.0	0.0
10.7	2.3	100.0	0.0	0.0	0.0
10.0	2.0	100.0	0.0	0.0	0.0
9.2	1.7	100.0	0.0	0.0	0.0
8.4	1.4	100.0	0.0	0.0	0.0
35.5	8.3	46.7	1.7	47.3	4.4
34.1	7.2	60.4	1.5	34.6	3.5
32.6	4.9	66.6	2.0	27.7	3.7
31.0	4.5	71.4	1.9	23.4	3.3
29.4	5.4	70.1	1.6	25.2	3.1
27.7	7.5	59.5	1.4	35.5	3.5
26.2	3.8	82.2	1.4	14.1	2.3
24.8	7.9	76.3	0.8	20.9	2.0
23.4	6.2	84.1	0.7	13.6	1.5
21.9	8.8	83.2	0.5	15.0	1.3
20.3	6.5	92.6	0.3	6.4	0.7
18.6	5.8	95.9	0.2	3.5	0.4
16.7	3.0	98.5	0.1	1.2	0.2
14.7	6.8	98.5	0.1	1.3	0.1
12.5	4.2	99.8	0.0	0.2	0.0
9.9	3.4	100.0	0.0	0.0	0.0

The applied total correction was less than 2% for the target foil in the 16MeV irradiation, where the cooling time was relatively short and the ^{99}Mo yield was low. The amount of the total correction depends on the cooling time and the magnitude of the cross section of the ^{99}Mo production process. With increasing proton energy the cross section of ^{99}Mo production is increasing therefore the required correction is larger. Applying a longer cooling time it also requires a larger relative correction as it can be seen for the 36.4MeV irradiation. Due to the relative high threshold energy for production of ^{90}Nb correction was made for the possible interfering E_γ=141.1keV gamma-line of ^{90}Nb above 20 MeV since no traces of the other strong E_γ=1129keV gamma-line was found the spectra at lower energies. The new results are included in Fig. 9 together with the recalculated results of our earlier experiment published in 2003 [12]. Numerical data are listed in table 4. To update the earlier reported values [12] the whole dataset was recalculated by using an interactive peak analysis this time (not relying on the automated peak analysis software routine) and by applying the same up to date decay parameters [24] and monitor reaction data as were used in this work. The recalculated dataset is indicated in light gray triangle in Fig. 9, while the new results, from the 16MeV and 36.4MeV irradiations, are represented by black dots. The original data, reported earlier in 2003, are lower about 10% than the recalculated ones. The recalculated cross section data supersede the data published earlier. It

is important to note that the three experiments were made independently using different irradiation setups, different detectors and different acquisition electronics and different standard gamma sources to determine the detector efficiency. Target foils were cut from the same sheet of a larger foil and the same data evaluation method and nuclear decay data as well as monitor reaction data were applied. As it is shown in Fig. 9 they have a very good overall agreement.
Numerical values of the original and recalculated cross section data of the ^{100}Mo(p,x)^{99}Mo and ^{100}Mo(p,2n)^{99m}Tc reactions for the Takacs 2003 publication [12] are given in Table 5.

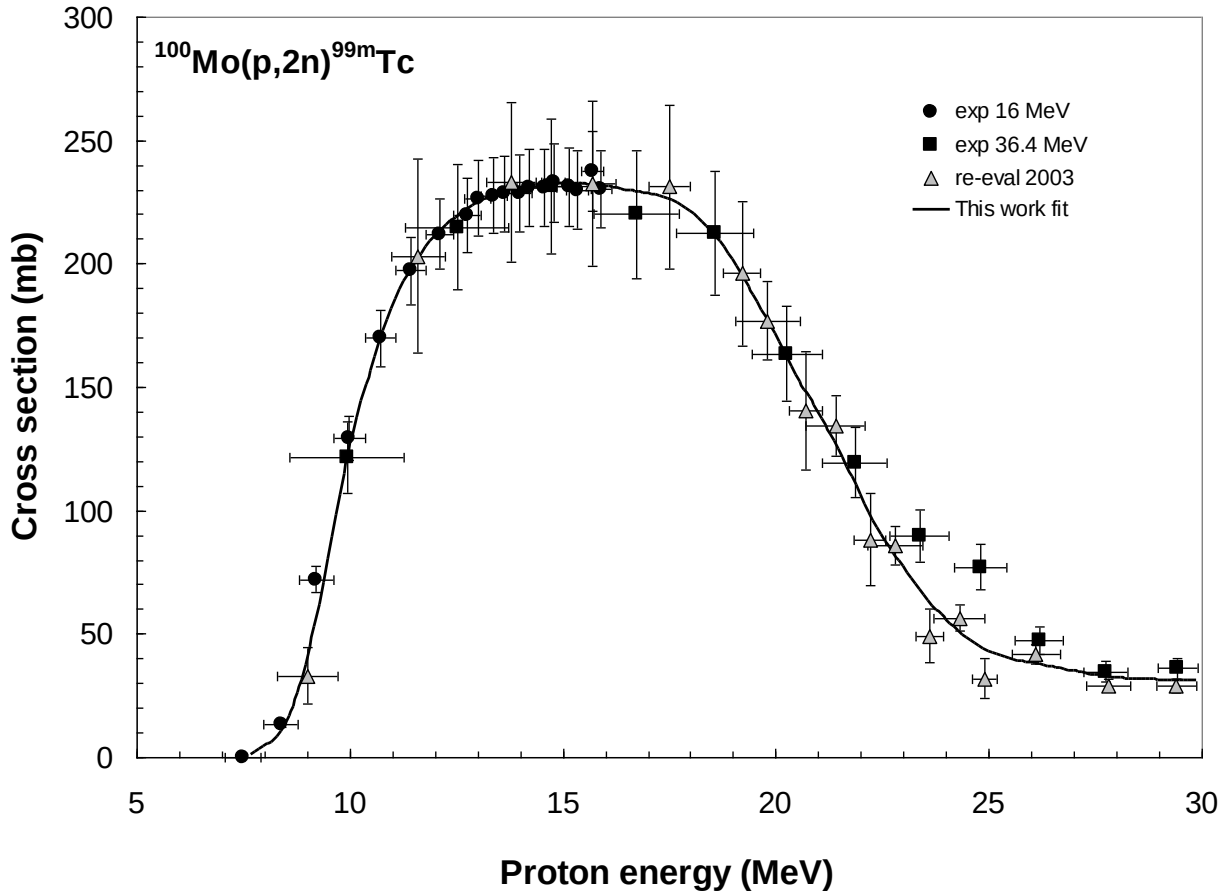

Fig. 9 The newly measured cross section values of the ^{100}Mo(p,2n)^{99m}Tc reaction in comparison with the recalculated earlier published data of Takacs 2003. The solid line is a spline fit of the results.

Table 4. Numerical values of the cross sections measured in this work normalized to 100% enriched ^{100}Mo target for the ^{100}Mo(p,2n)^{99m}Tc and for the cumulative cross sections for the ^{100}Mo(p,x)^{99}Mo reactions. Data from the E_p=16MeV and E_p=36.4MeV irradiations are combined and presented as one experiment.

	^{100}Mo(p,2n)^{99m}Tc	^{100}Mo(p,x)^{99}Mo
Energy MeV	Sigma mb	Sigma mb
35.54 ± 0.32	25.4 ± 3.0	185.8 ± 16.5

34.09	±	0.35	34.2	±	4.0	180.6	±	16.3
32.60	±	0.39	28.8	±	3.4	181.6	±	16.8
31.04	±	0.43	35.7	±	4.2	183.0	±	17.8
29.42	±	0.47	36.0	±	4.3	174.9	±	17.4
27.73	±	0.51	34.8	±	4.1	178.8	±	16.6
26.18	±	0.57	47.5	±	5.6	169.8	±	15.5
24.80	±	0.62	77.1	±	9.1	169.1	±	15.3
23.37	±	0.68	89.7	±	10.6	165.0	±	16.5
21.85	±	0.75	119.4	±	14.1	148.0	±	13.6
20.26	±	0.83	163.6	±	19.4	120.3	±	13.0
18.56	±	0.91	212.6	±	25.2	94.8	±	9.2
16.73	±	1.00	220.1	±	26.0	68.4	±	10.2
15.89	±	0.25	230.2	±	15.6	41.9	±	3.88
15.68	±	0.25	237.5	±	16.2	38.4	±	3.44
15.35	±	0.26	230.0	±	15.7	33.2	±	4.34
15.13	±	0.27	231.2	±	15.7	30.3	±	2.78
14.78	±	0.27	232.8	±	15.9	25.2	±	2.79
14.74	±	1.10	231.6	±	27.4	30.6	±	5.4
14.56	±	0.28	230.8	±	15.7	24.1	±	1.34
14.21	±	0.29	230.7	±	15.7	18.4	±	2.99
13.97	±	0.29	228.8	±	15.6	17.3	±	3.11
13.61	±	0.30	228.4	±	15.5	12.6	±	1.17
13.37	±	0.30	227.7	±	15.5	11.6	±	1.29
13.00	±	0.31	226.6	±	15.2	5.8	±	0.69
12.75	±	0.32	219.7	±	14.9	7.9	±	2.69
12.51	±	1.21	214.7	±	25.4	7.4	±	5.6
12.10	±	0.33	212.2	±	14.4			
11.43	±	0.35	197.2	±	13.4	5.4	±	0.73
10.72	±	0.36	169.9	±	11.5			
9.99	±	0.38	129.6	±	8.9			
9.93	±	1.33	121.6	±	14.4			
9.21	±	0.40	72.2	±	5.1			
8.38	±	0.41	13.3	±	1.3			

Table 5. The original and the recalculated cross section data of the $^{100}Mo(p,x)^{99}Mo$ and $^{100}Mo(p,2n)^{99m}Tc$ reactions in the Takacs 2003 experiment [12].

	$^{100}Mo(p,x)^{99}Mo$	$^{100}Mo(p,2n)^{99m}Tc$	$^{100}Mo(p,x)^{99}Mo$	$^{100}Mo(p,2n)^{99m}Tc$
Energy MeV	Sigma mb	Sigma mb	Sigma re-eval mb	Sigma re-eval mb
5.7 ± 0.78		0.7 ± 0.7		
9.0 ± 0.71		34.7 ± 11.5	2.0 ± 2.6	33.0 ± 11.5
11.6 ± 0.64		173.5 ± 39.2	3.6 ± 0.6	203.2 ± 39.2
13.8 ± 0.58	15.7 ± 1.5	205.8 ± 32.5	17.7 ± 2.0	233.1 ± 32.5

15.7	±	0.53	51.2	±	6.3	211.2	±	33.4	45.4	±	5.1	232.6	±	33.4
17.5	±	0.48	73.6	±	7.9	208.3	±	33.4	75.8	±	8.5	231.2	±	33.4
19.2	±	0.44	110.2	±	12.9	184.6	±	29.4	104.7	±	11.8	196.0	±	29.4
19.8	±	0.76	120.1	±	15.3	163.2	±	18.3	119.6	±	13.2	176.9	±	15.9
20.7	±	0.40	137.6	±	16.0	150.9	±	24.1	130.6	±	14.7	140.5	±	24.1
21.4	±	0.70	146.6	±	20.5	113.4	±	12.7	130.3	±	14.4	134.5	±	12.1
22.2	±	0.36	161.7	±	19.2	113.5	±	18.7	152.9	±	17.2	88.3	±	18.7
22.8	±	0.65	171.3	±	22.5	91.7	±	10.3	154.8	±	17.2	85.9	±	7.7
23.6	±	0.33	174.4	±	20.2	63.5	±	10.8	164.5	±	18.5	49.2	±	10.8
24.3	±	0.60	179.0	±	29.1	45.5	±	5.1	167.9	±	18.6	56.6	±	5.1
24.9	±	0.30	179.8	±	20.3	49.7	±	8.1	173.0	±	19.4	31.8	±	8.1
26.1	±	0.56	174.1	±	26.0	33.4	±	3.7	173.4	±	19.2	41.8	±	3.8
27.8	±	0.51	173.3	±	20.9	18.3	±	2.1	175.9	±	19.5	29.2	±	2.6
29.4	±	0.48	178.5	±	24.0	17.1	±	1.9	179.4	±	19.9	29.0	±	2.6
31.0	±	0.44	178.8	±	20.5	14.5	±	1.6	175.1	±	19.4	27.7	±	2.5
32.5	±	0.41	179.4	±	26.8	17.1	±	1.9	182.1	±	20.2	28.2	±	2.5
33.9	±	0.38	178.0	±	23.4	21.0	±	2.4	184.6	±	20.5	20.1	±	1.8
35.3	±	0.35	180.0	±	23.2	15.4	±	1.7	182.5	±	20.2	22.6	±	2.0
36.5	±	0.32	177.4	±	24.0	21.5	±	2.4	179.1	±	19.8	9.0	±	0.8
37.9	±	0.30	177.4	±	21.9	20.9	±	2.3	178.5	±	19.8	6.8	±	0.6

5. Results and discussion

The ^{100}Mo(p,2n)^{99m}Tc reaction is one of the proposed processes for direct production of ^{99m}Tc. Among the suggested possible alternative production methods of ^{99m}Tc the direct production using the ^{100}Mo(p,2n) reaction on highly enriched ^{100}Mo target material appears to be very promising. Using this production method several additional activation products are expected in the irradiated target with different activity levels depending on the actual enrichment level of the ^{100}Mo target material, on the bombarding proton energy and on irradiation time. The relative importance of the possible contributing reactions and their respective contribution to the total activity and the patient dose can be theoretically estimated, once known the products yielding occurrences. The knowledge of the ^{100}Mo(p,2n)^{99m}Tc excitation function has a basic role. However, the available datasets are quite discrepant. There is an amplitude difference between the lowest and the highest datasets more than a factor of two. Due to the relative complexity of the ^{99}Mo and ^{99m}Tc decay a correction on the individual datasets is only possible if all the experimental parameters were available. None of the publication contains these parameters completely; therefore proper correction of the dataset is impossible. Using well controlled experimental conditions and the latest decay parameters of the ^{99}Mo and ^{99m}Tc radionuclide pair we have re-measured the cross section of the ^{100}Mo(p,2n)^{99m}Tc reaction. The new cross section points were deduced in experimental conditions where the possible systematic error sources were minimized. Well defined shiny surface metallic thin Mo foils with natural isotopic composition were used as targets for which the numbers of target atoms were determined with an uncertainty less than 1%. The average absolute beam intensity calculated from the collected charge was compared to the value deduced from the recommended cross sections of the ^{nat}Ti(p,x)^{48}V monitor reaction. The direct measured beam intensity was 2.5% higher than the value deduced from the monitor reaction. In the cross section calculation process, the beam current derived from monitor reaction was adopted. The applied detector efficiency curves were cross checked by using

different energy gamma lines of the same radionuclide in the analysis. Almost identical values were received by using the E_γ=739.5keV gamma-line and the low energy E_γ=140.5keV gamma-line of ^{99}Mo in equilibrium for determining the cross section of the ^{100}Mo(p,x)^{99}Mo process, which proved the shape of the used detector efficiency curve. Also results for other non interfering nuclear reactions were compared with earlier published data and good agreements were found which provides an overall confirmation of the experiment. As examples the cross section of the ^{nat}Mo(p,x)^{95m}Tc and ^{nat}Mo(p,x)^{96g}Tc processes were calculated using non-interfering gamma-lines and are given in Fig. 10 and Fig. 11. A good agreement among the independently measured datasets [8, 16, 19, 32, 33] can be seen in Fig. 10 and in Fig 11. This agreement proves that the main discrepancy among the published experimental cross section data of the ^{100}Mo(p,2n)^{99m}Tc could originate from the data evaluation methods. Another control of the data evaluation method was the re-evaluation of the result of our independent experiment published in 2003. The re-evaluated data of that experiment agrees with data of this work well. All these can confirm the results of the new experiment regarding the deduced cross sections for the ^{100}Mo(p,2n)^{99m}Tc reaction.

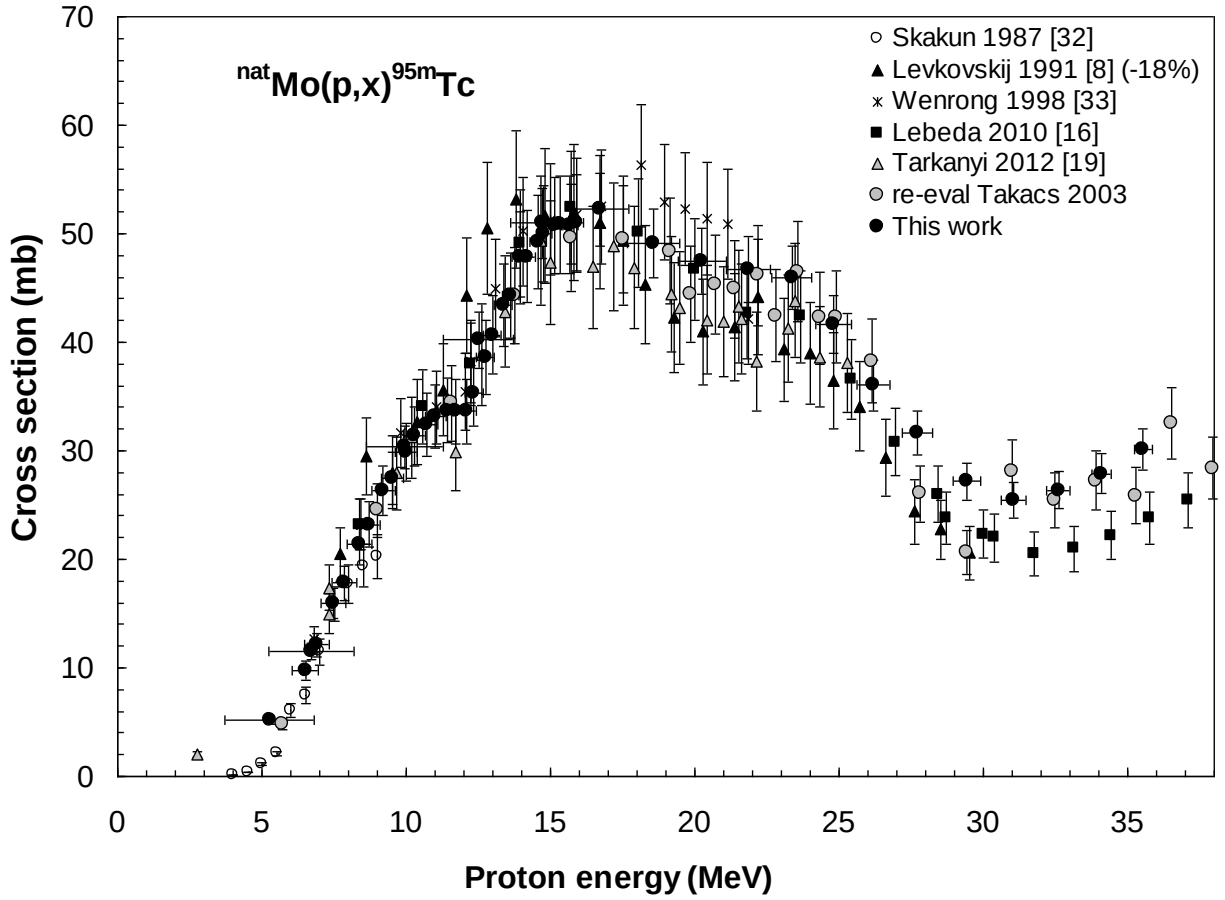

Figure 10. Cross section data deduced for the ^{nat}Mo(p,x)^{95m}Tc process in comparison with data reported earlier. Data are in good agreement which gives an overall confirmation of this experiment.

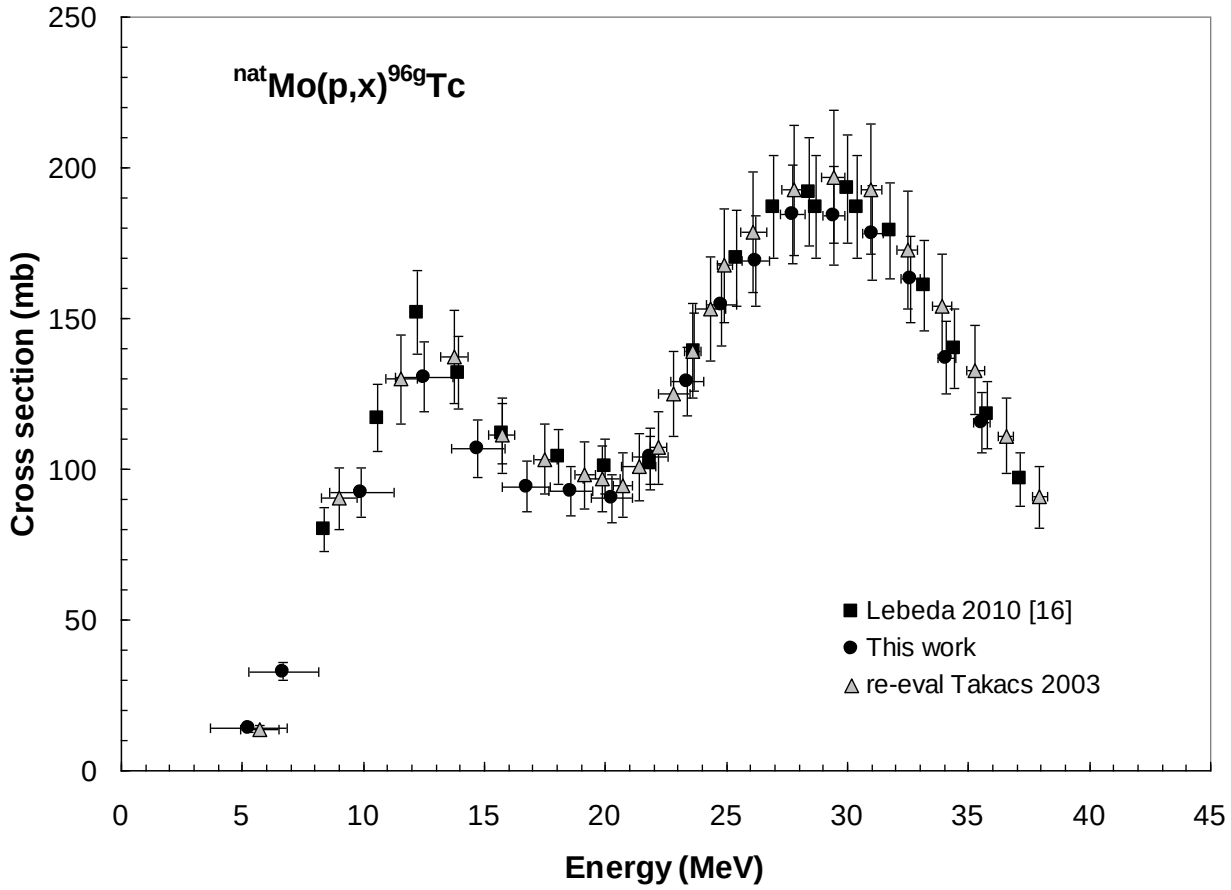

Figure 11. Cross section data deduced for the $^{nat}Mo(p,x)^{96g}Tc$ process in comparison with data reported earlier. Data are in good agreement that gives an overall confirmation of this latest experiment.

6. Conclusion

We have determined experimentally the excitation function of the $^{100}Mo(p,x)^{99}Mo$ and $^{100}Mo(p,2n)^{99m}Tc$ reactions using analytically derived equations in the data evaluation and found a good agreement among the results of independently performed three irradiations. This agreement proves that the main discrepancy among the published experimental cross section data of the $^{100}Mo(p,2n)^{99m}Tc$ reaction could originate from the data evaluation methods. A spline fit was calculated using the newly measured two data sets and the re-evaluated data of 2003 experiment. Numerical values of the fit are collected in Table 6.

In Fig. 12 results of the E_p=16MeV and E_p=36.4MeV irradiations are combined and presented as one experiment in comparison with the results published earlier. The two theoretical calculations taken from TENDL2013 data library [34] and the recent paper of Qaim [23] are disagree from the experimental results in different ways regarding the shape and amplitude of the curves. Calculation of the evaluated excitation function presented by Qaim et al. [23] based on nuclear model codes TALYS and STAPRE using input parameters adjusted to selected experimental data, within their recommended limits. By using input parameters that way, they have included datasets in their evaluation with considerable different amplitudes, therefore their result describes more or less a kind of average of the experimental data. The excitation function proposed by

Qaim et al. [23] is higher at the maximum and show asymmetrical shape around the maximum with higher values at higher energy. While the result of the a-priory TALYS calculation provided lower cross sections with asymmetrical shape around the maximum with higher values at lover energy.

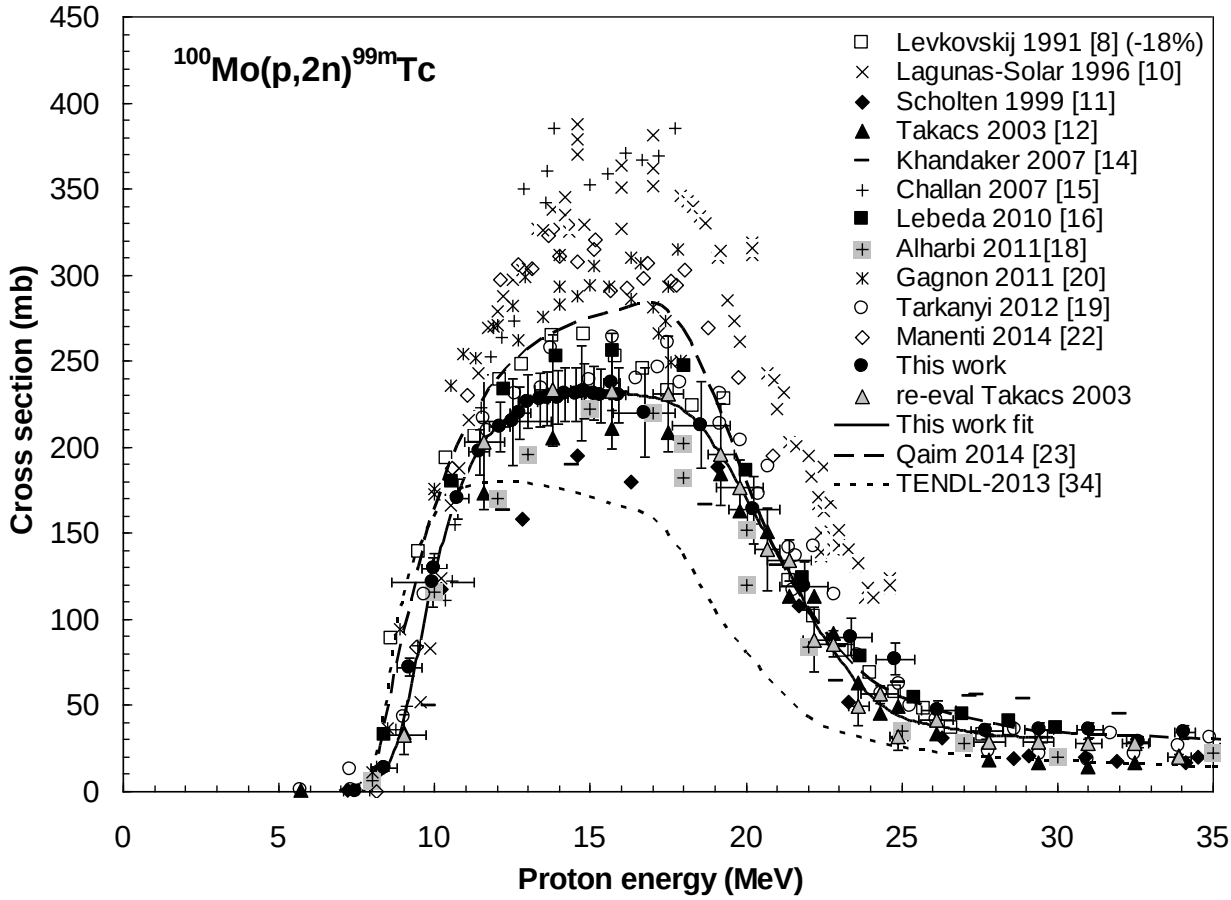

Figure 12. The newly measured cross section data of the ^{100}Mo(p,2n)^{99m}Tc reaction in comparison with data reported earlier. The thick solid line is a spline fit of the results of this work and the re-evaluated data of [12].

There are several experimental cross section data sets available for the ^{100}Mo(p,2n)^{99m}Tc reaction measured on enriched and natural Mo targets including ours. These valuable data are result of significant efforts of authors. Considering all the available data sets, Lebeda's data and our new results (results from three independent experiments) provided smoothest curves with relative small scatter. We are convinced that a smooth curve confirms that the experiment is done in a well controlled manner and the deduced data may not contain large additional unknown systematic error. In each experiment (our three independent experiments and in Lebeda's work too [private communication]) the whole excitation function of the used monitor reaction was re-measured with very good agreement, which confirmed the validity of the experimental technique. By analyzing the possible error sources we designed the experiment such a way that the error sources were minimal or eliminated. A smooth curve indicates that at least those possible error

sources which could result in scatter of the measured cross section data were properly handled (first of all activity measurements and data evaluation method).

Table 6. Spline fit of the combined results of this work and the re-evaluated data of [12].

Energy MeV	Sigma mb	Energy MeV	Sigma mb
8.0	3.4	23.0	77.4
9.0	37.2	24.0	56.0
10.0	123.0	25.0	43.2
11.0	181.7	26.0	38.3
12.0	210.8	27.0	35.0
13.0	224.5	28.0	32.3
14.0	230.8	29.0	31.5
15.0	232.5	30.0	31.3
16.0	231.4	31.0	30.7
17.0	228.5	32.0	29.3
18.0	221.5	33.0	27.1
19.0	201.8	34.0	25.0
20.0	171.6	35.0	22.5
21.0	140.1	36.0	14.8
22.0	106.4	37.0	7.8

Acknowledgement

This work was carried out in the frame of the standing HAS-JSPS (Hungary–Japan) bilateral exchange agreement. The authors acknowledge the support of the respective institutions in providing technical support and use of experimental facilities. (Contract No.: NKM-89/2014)

References

1 IAEA, *Non-HEU Production Technologies for Molybdenum-99 and Technetium-99m*; Nuclear Energy Series: No. NF-T-5.4, IAEA, Vienna, 2013

2 IAEA, *Technetium-99m Radiopharmaceuticals: Status and Trends*, IAEA Radioisotopes and Radiopharmaceuticals Series, No. 1, IAEA, Vienna, 2009

3 OECD NEA, *The supply of Medical Radioisotopes: Review of Potential Molybdenum-99/Technetium-99m Production Technologies*, NEA, Nuclear development, November 2010, Paris,

4 National Research Council: *Medical Isotope Production Without Highly Enriched Uranium.* Washington, DC: National Academies Press; 2009: 69.

5 F. Bénard, K.R. Buckley, T.J. Ruth, S.K. Zeisler, J. Klug, V. Hanemaayer, M. Vuckovic, Xinchi Hou, A. Celler, J-P. Appiah, J. Valliant, M.S. Kovacs and P. Schaffer, *Implementation of Multi-Curie Production of ^{99m}Tc by Conventional Medical Cyclotrons.* Journal of Nuclear Medicine, 55 (2014) 1017-1022.

6 IAEA CRP F22062, *Accelerator-based Alternatives to Non-HEU Production of ^{99}Mo/^{99m}Tc*, , http://cra.iaea.org/crp/project/ProjectDetail?projectId=1862&lastActionName=AllActiveCRPList

7 J. Beaver, H. Hupf, *Production of ^{99m}Tc on a medical cyclotron: A feasibility study.* J. Nucl. Med. 12 (1971) 739–41.

8 V.N. Levkovskij :Middle mass nuclides (A=40–100) activation cross-sections by medium energy (E=10–50 MeV) protons and alpha particles (experiment and systematics), Inter-vesi, Moscow, 1991.

9 M.C. Lagunas-Solar, P.M. Kiefer, O.F. Carvacho, C.A. Lagunas, Y.P. Cha, *Cyclotron production of NCA ^{99m}Tc and ^{99}Mo an alternative non-reactor supply of instant ^{99m}Tc and ^{99}Mo/^{99m}Tc generator.* Appl. Radiat. Isot.42 (1991) 643–657.

10 M.C. Lagunas-Solar, N.X. Zeng, I. Mirshad, T. Grey-Morgan , *An Update on the Direct Production of 99mTc with Proton Beams and Enriched 100Mo Targets*, Journal of American Nucl. Soc. 74(1996)137 (also in: *Accelerator production of ^{99m}Tc with proton beams and enriched ^{100}Mo targets*, IAEA-TECDOC-1065. p 95, IAEA, Vienna, 1999.)

11 B. Scholten, R.M. Lambrecht, M. Cogneau, H. VeraRuiz, *Excitation functions for the cyclotron production of ^{99m}Tc and ^{99}Mo.* Appl.Radiat.Isot. 51 (1999) 69–80.

12 S. Takács, Z. Szűcs, F. Tárkányi, A. Hermanne, M. Sonck, *Evaluation of proton induced reactions on ^{100}Mo: new cros ssections for production of ^{99m}Tc and ^{99}Mo.* J.Radioanal.Nucl.Chem.257 (2003),195–201.

13 M.S. Uddin, M. Hagiwara, F. Tarkanyi, F. Ditroi, M. Baba, *Experimental studies on the proton-induced activation reactions of molybdenum in the energy range 22–67MeV.,* Appl. Radiat. Isot. 60(6)(2004) 911–920.

14 M.U. Khandaker, M.S. Uddin, K.S. Kim, Y.S. Lee, G.N. Kim, *Measurement of cross-sections for the (p,xn) reactions in natural molybdenum.* Nucl. Instrum. Methods in Phys. Res. B262 (2) (2007) 171–181.

15 M. Challan, M. Comsan, M. Abou-Zeid, *Thin target yields and EMPIRE-II predictions on the accelerator production of technetium-99m.* Nucl. Rad. Phys.2 (2007) 1–12.

16 O. Lebeda, M. Pruszyński. *New measurement of excitation functions for (p,x) reactions on ^{nat}Mo with special regard to the formation of ^{95m}Tc, $^{96m+g}$Tc, ^{99m}Tc and ^{99}Mo.* Appl. Radiat. Isot. 68 (2010)55–65

17 P. Chodash, C.T. Angell, J. Benitez, E.B. Norman, M. Pedretti, H. Shugart, E. Swanberg, R. Yee, *Measurement of excitation functions for the ^{nat}Mo(d,x)^{99}Mo and ^{nat}Mo(p,x)^{99}Mo reactions.* Appl. Radiat. Isot. 69 (2011) 1447-1452.

18 A.A. Alharbi, A. Azzam, M. McCleskey, B. Roeder, A. Spiridon, E. Simmons, V.Z. Goldberg, A. Banu, L. Trache, R.E. Tribble, *Medical radioisotopes production: comprehensive cross section study for the production of Mo and Tc radioisotopes via proton induced nuclear reactions on ^{nat}Mo,* in Radioisotopes Applications in Biomedical Science, N. Singh (Ed.), ISBN: 978-953-307-748-2, 2011, intechopen.com/books

19 F. Tárkányi, F. Ditrói, A. Hermanne, S. Takács, A.V. Ignatyuk, *Investigation of activation cross sections of proton induced nuclear reactions on ^{nat}Mo up to 40 MeV: new data and evaluations.* Nucl. Instr. Meth. B280 (2012) 45-73.

20 K. Gagnon, F. Bénard, M. Kovacs, T.J. Ruth, P. Schaffer, J.S. Wilson, S.A. McQuarrie, 2011. *Cyclotron production of ^{99m}Tc: Experimental measurement of the ^{100}Mo(p,x)^{99}Mo, ^{99m}Tc and ^{99g}Tc excitation functions from 8 to 18 MeV.* Nucl. Med. Biol., 38 (2011) 907-916.

21 M.U. Khandaker, A.K.M.M.H. Meaze, K. Kim, D. Son, G. Kim, *Measurements of the proton-induced reaction cross sections of ^{nat}Mo by using the MC50 cyclotron at the Korea Institute of Radiological and Medical Sciences*. J. Korean Phys. Soc. 48 (2006) 821-826.

22 S. Manenti, U. Holwarth, M. Loriggiola, L. Gini, J, Esposito, F. Groppi, F. Simonelli, *The excitation functions of ^{100}Mo(p,x)^{99}Mo and ^{100}Mo(p,2n)^{99m}Tc,* Appl. Radiat. Isot. 94 (2014)344–348

23 S.M. Qaim, S. Sudár, B. Scholten, A.J. Koning, H.H. Coenen, *Evaluation of excitation functions of ^{100}Mo(p,d+pn)^{99}Mo and ^{100}Mo(p,2n)^{99m}Tc reactions: Estimation of long-lived Tc-impurity and its implication on the specific activity of cyclotron-produced ^{99m}Tc,* Applied Radiation and Isotopes 85 (2014) 101–113.

24 M.M. Bé, V. Chisté, C. Dulieu, V. Chechev, N. Kuzmenko, R. Helmer, A. Nichols, E. Schönfeld, R. Dersch, *Monographie BIPM-5*, Table of Radionuclides, Vol. 1, A=1 to 150, 2004, Ed. BIPM, France

25 Nuclear structure and decay data on-line library, Nudat 2.6, National Nuclear Data Center, Brookhaven National Laboratory, USA, URL: http://www.nndc.bnl.gov/nudat2/

26 Q-value Calculator (QCalc), http://www.nndc.bnl.gov/qcalc/

27 M.E. Wieser and M. Berglund, *Atomic weights of the elements 2007*, Pure Appl. Chem., Vol. 81, No. 11, 2009, pp. 2131–2156, doi:10.1351/PAC-REP-09-08-03 (IUPAC Technical Report)

28 G. Székely, *FGM — A flexible gamma-spectrum analysis program for a small computer*, Comp. Phys. Comm. 34 (1985) 313.

29 H.H. Andersen, J.F. Ziegler, 1977. *Hydrogen Stopping powers and ranges in all elements*, Volume 3 of the Stopping and ranges of ions in matter, Pergamon Press, ISBN 0-08-021605-6.

30 IAEA-TECDOC-1211, *Charged particle cross section database for medical radioisotope production. Beam Monitor Reactions (Chapter 4)*, IAEA-TECDOC-1211, Vienna, 2001, URL: http://www-nds.iaea.org/medical/monitor_reactions.html

31 CRP on *Nuclear Data for Charged-particle Monitor Reactions and Medical Isotope Production*, Duration: 2012-2016; CRP Code: F4.10.29; IAEA Project Officer: R. Capote

32 E.A. Skakun, V.G. Batij, Yu.N. Rakivnenko, O.A. Rastrepin, *Excitation functions and isomer ratios for up-to-9 MeV proton interactions with Zr and Mo isotope nuclei.* Jour: Yadernaya Fizika, 46, (1987) 28, (Eglish translation: Sov. J. Nucl. Phys. 46 (1987) 17).

33 Z. Wenrong, Yu. Weixiang, H. Xiaogang, Lu. Hanlin, *Communication of Nuclear Data Progress* (CNIC-01266,CNDC-0022), 1998, vol.19,p.17.

34 A.J. Koning and D. Rochman**;** *TENDL-2013: TALYS-based Evaluated Nuclear Data Library.* Nuclear Research and Consultancy Group (NRG) Petten, The Netherlands, Release date: December 23, 2013, URL: http://www.talys.eu/tendl-2013/